Journal Pre-proof

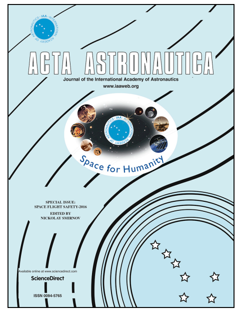

An anchored space elevator under the L1 Mars-Phobos libration point

Vladimir S. Aslanov

PII: S0094-5765(25)00314-5

DOI: https://doi.org/10.1016/j.actaastro.2025.05.032

Reference: AA 11170

To appear in: *Acta Astronautica*

Received Date: 11 April 2025

Revised Date: 17 May 2025

Accepted Date: 18 May 2025

An anchored space elevator under the L1 Mars-Phobos libration point

Vladimir S. Aslanov[1,*]

Moscow Aviation Institute (National Research University), 4, Volokolamskoe shosse, Moscow, A-80, GSP-3, 125993, Russia

Abstract

The paper studies the dynamics of a space elevator deployed from the surface of Phobos towards Mars. The space elevator consists of a space station and a climber that can move along the elevator's tether. The motion of the system occurs under the conditions of a planar elliptic restricted three-body problem. Two different system configurations are considered. In both of them, the station is located above the L1 libration point. In the first case, the climber can move between Phobos and the station, and in the second case, the climber attached to the end of the tether can move from the station in the direction of Mars and from Mars to the station direction. The second configuration of space elevator can be used as a stationary probe (in the Local-Vertical-Local-Horizontal frame), fixed at a given distance between Mars and Phobos, and as a means of launching a probe on a fly-around trajectory and a descent trajectory to the surface of Mars.

Keywords: L1 libration point; anchored space elevator; Phobos surface; equations of motion.

1. Introduction

Future missions to explore planets and their moons in the solar system may utilize space tether systems and space elevators as an alternative to jet propulsion systems. The concept of a space elevator was proposed more than 100 years ago by Tsiolkovsky [1]. The design of the space elevator was developed by Arnautov [2]. Pearson investigated the problems of buckling, strength, and dynamic stability of an "orbital tower" connecting the Earth's surface to geostationary [3]. The theoretical

* Corresponding author

[1] E-mail address: aslanov_vs@mail.ru. Website: http://aslanov.ssau.ru

aspects of the development of space elevators and tethered systems as the basis for space elevators are the subject of a large number of works, including those by Beletsky, Levin, Misra, Zhu and others [4-31]. The basis of the Earth's Space Elevator is an approximately 100,000 kilometres long tether attached to the Earth's surface. Of course, such a design could be built in the distant future, although some scientists are more optimistic. A more realistic task looks like building a space elevator to explore the Mars' moon, Phobos. The fact that the distance between the surfaces of Mars and Phobos is about 6 thousand kilometres, and that Phobos always faces one way towards Mars. Note that in the Mars-Phobos system the L1 collinear libration point is located only 3.4 km from the surface of Phobos, and if the centre of mass of a space elevator anchored to Phobos, consisting of a station, a climber and a tether, is always further than the L1 point of Phobos, then it can be expected that the tether will be stretched as the climber moves. Only numerical and analytical calculations can determine this more precisely. Nevertheless, it follows that the space elevator anchored on Phobos and directed towards Mars could have a length of about 5-6 km to 6 thousand km. These two circumstances make the building of such a space elevator a feasible project in the not too distant future. Such a project could form the basis of many missions to explore Phobos, Mars and the space around them.

Some theoretical work has already been done on the exploration of Phobos using tethered systems and space elevators [29, 32-34]. At the same time, the issue of building a space elevator anchored on Phobos and deployed towards Mars is considered for the first time.

The aim of the work is to demonstrate the feasibility of building a space elevator anchored to Phobos and deployed towards Mars. To achieve this aim, a mathematical model of the space elevator is derived in the context of a planar elliptic restricted three-body problem, and a control law for the climber's motion is chosen to ensure that the tether does not become slack. Two configurations of the space elevator are considered: the first, classical, where the climber moves between the surface of Phobos and a station located above the L1 libration point; in the second case, the end-body moves from the station towards Mars. The second configuration explores the additional option of having the climber or probe separate from the tether at the endpoint and then orbit Mars or descend to the surface of Mars.

2. Mathematical models and methods

The following acceptable assumptions are introduced:

1. It is supposed that the primaries move in elliptical orbits around their mutual mass center (point O in Fig. 1). The distance between the primaries changes over time and is determined by the expression

$$r = \frac{p}{1+e\cos f} \tag{1}$$

Where f is the true anomaly, p is the semilatus rectum, e is the eccentricity of the orbit.

2. The space elevator is considered as a double pendulum. The masses of the climber m_1 and the station m_2 are significantly smaller than the primary masses M_1 and M_2

$$m_1,\, m_2 \ll M_2 < M_1 \tag{2}$$

3. The double pendulum consist of weightless rigid rods of variable length l_1, l_2.

4. In the elliptical restricted three-body problem, the mean rotation is

$$\frac{df}{dt} = \frac{\sqrt{G\left(m_1+m_2\right)p}}{r^2} \tag{3}$$

where G is Newtonian gravitational constant.

Consider the planar motion of the space elevator in gravitational fields created by two primaries in the Local-Vertical-Local-Horizontal frame Oxy (Fig. 1) within the scope of the elliptic restricted three-body problem [35]

$$\ddot{x}_1 - \dot{f}^2 x_1 - 2\dot{f}\,\dot{y}_1 - \ddot{f}\,y_1 = \frac{1}{m_1}\left[\frac{\partial U}{\partial x_1} + T_{1x} + T_{2x}\right], \tag{4}$$

$$\ddot{y}_1 - \dot{f}^2 y_1 + 2\dot{f}\,\dot{x}_1 + \ddot{f}\,x_1 = \frac{1}{m_1}\left[\frac{\partial U}{\partial y_1} + T_{1y} + T_{2y}\right], \tag{5}$$

$$\ddot{x}_2 - \dot{f}^2 x_2 - 2\dot{f}\,\dot{y}_2 - \ddot{f}\,y_2 = \frac{1}{m_2}\left[\frac{\partial U}{\partial x_2} + T_{2x}\right], \tag{6}$$

$$\ddot{y}_2 - \dot{f}^2 y_2 + 2\dot{f}\,\dot{x}_2 + \ddot{f}\,x_2 = \frac{1}{m_2}\left[\frac{\partial U}{\partial y_2} + T_{2y}\right] \tag{7}$$

where $\mathbf{T}_i = \left(T_{ix}, T_{iy}\right)$ are the tether tension forces ($i = 1, 2$), l_1 and l_2 are the lengths of the tethers 1 and 2, respectively. The potential of Eqs. (4) and (5) can be written in the following form

$$U(x_1, y_1, x_2, y_2) = G\left(\frac{m_1 M_1}{r_{11}} + \frac{m_1 M_2}{r_{12}} + \frac{m_2 M_1}{r_{21}} + \frac{m_2 M_2}{r_{22}}\right) \tag{8}$$

Here m_i is the mass of the i-th point, M_1 is the mass of Mars, M_2 is the mass of Phobos; the distances from the primaries to the climber and the space station are defined as (Fig. 1)

$$r_{11} = \sqrt{(x_1 + \mu r)^2 + y_1^{\,2}}\,, \qquad r_{12} = \sqrt{(x_1 - \nu r)^2 + y_1^{\,2}} \tag{9}$$

$$r_{21} = \sqrt{(x_2 + \mu r)^2 + y_2^{\,2}}\,, \qquad r_{22} = \sqrt{(x_2 - \nu r)^2 + y_2^{\,2}} \tag{10}$$

$$\mu = \frac{M_2}{M_1 + M_2}, \qquad \nu = \frac{M_1}{M_1 + M_2} = 1 - \mu \tag{11}$$

where μ and ν are the mass ratios ($0 < \mu \le 0.5$, $0.5 \le \nu < 1$).

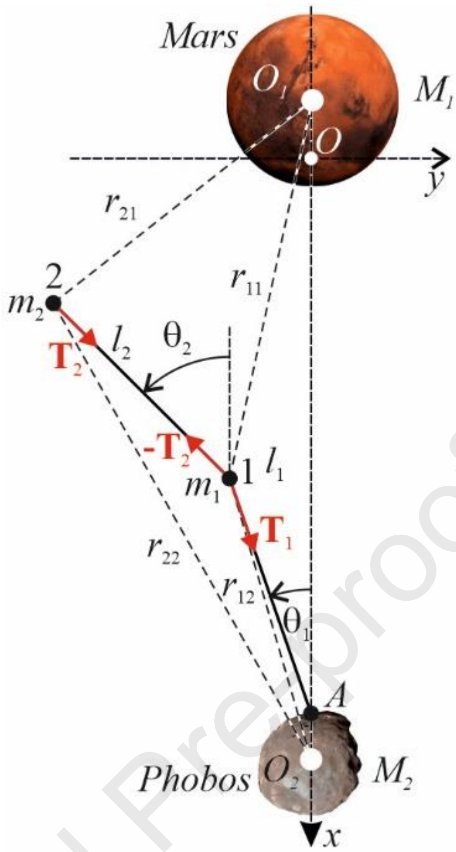

Fig. 1. The frame Oxy.

The substitution of Nechvile's variables

$$x_i = r\xi_i, \qquad y_i = r\eta_i \qquad\qquad (i = 1, 2) \tag{12}$$

reduces Eqs. (4)-(7) to dimensionless form [35, 36]

$$\xi_1'' - 2\eta_1' = \frac{1}{k}\frac{\partial\Omega}{\partial\xi_1} + \frac{1}{m_1}\bar{T}_{1x}, \tag{13}$$

$$\eta_1'' + 2\xi_1' = \frac{1}{k}\frac{\partial\Omega}{\partial\eta_1} + \frac{1}{m_1}\bar{T}_{1y}, \tag{14}$$

$$\xi_2'' - 2\eta_2' = \frac{1}{k}\frac{\partial\Omega}{\partial\xi_2} + \frac{1}{m_2}\bar{T}_{2x}, \tag{15}$$

$$\eta_2'' + 2\xi_2' = \frac{1}{k}\frac{\partial \Omega}{\partial \eta_2} + \frac{1}{m_2}\overline{T}_{2y} \tag{16}$$

where $k = 1 + e\cos f$, $(.)' = \dfrac{d}{df}(.)$ and $(.)'' = \dfrac{d^2}{df^2}(.)$, $\overline{\mathbf{T}}_i$ is the vector of dimensionless tether tension force, Ω is the potential function defined as

$$\Omega = \frac{1}{2}\left(\xi_1^2 + \xi_2^2 + \eta_1^2 + \eta_2^2\right) + \nu\left(\frac{1}{\rho_{11}} + \frac{1}{\rho_{21}}\right) + \mu\left(\frac{1}{\rho_{12}} + \frac{1}{\rho_{22}}\right) \tag{17}$$

$$\rho_{i1} = \sqrt{\left(\xi_i + \mu\right)^2 + \eta_i^2}, \qquad \rho_{i2} = \sqrt{\left(\xi_i - \nu\right)^2 + \eta_i^2} \qquad \left(i = 1,2\right) \tag{18}$$

$$\overline{\mathbf{T}}_i = (\overline{T}_{ix}, \overline{T}_{iy}) = \frac{p^3}{m_i C^2 k^3}\mathbf{T}_i \;\; C = \sqrt{G\left(M_1 + M_2\right)p} \tag{19}$$

The position of the tether anchor point A is entered by the dimensionless coordinate

$$\sigma = \nu - \frac{a}{p}k, \tag{20}$$

where a is the coordinate of the anchored point A in the frame Oxy (Fig. 1). Position of the 1-point and the 2-point relative to the point A can be defined as

$$\xi_1 = \sigma - \lambda_1\cos\theta_1, \qquad \eta_1 = -\lambda_1\sin\theta_1 \tag{21}$$

$$\xi_2 = \sigma - \left(\lambda_1\cos\theta_1 + \lambda_2\cos\theta_2\right), \quad \eta_2 = -\left(\lambda_1\sin\theta_1 + \lambda_2\sin\theta_2\right) \tag{22}$$

Here θ_1 and θ_2 are the angles of deflection of tethers l_1 and l_2 from the line connecting the primaries (Fig.1). The dimensionless lengths of the tethers are

$$\lambda_1 = \frac{l_1}{r} = \frac{l_1}{p}k, \qquad \lambda_2 = \frac{l_2}{r} = \frac{l_2}{p}k \tag{23}$$

The transition from Cartesian to polar coordinates can be made using the expressions (21), (22) in Eqs. (13)-(16)

$$p\lambda_1\theta_1'' = \frac{ae}{2}\left(3\sin\left(f-\theta_1\right)+\sin\left(f+\theta_1\right)\right)+\frac{\sin\theta_1}{k}\left(p\nu-ak+\frac{\nu\left(-p+ak\right)}{\rho_{11}^3}+\frac{\mu k}{\rho_{12}^3}\right)-$$

$$2p\left(1+\theta_1'\right)\lambda_1'-\frac{p^4}{C^2k^3m_1}T_2\sin\theta_{12}, \tag{24}$$

$$p\lambda_2\theta_2'' = \frac{1}{k}\left[\mu\left(ak\sin\theta_2-p\lambda_1\sin\theta_{12}\right)\left(-\frac{1}{\rho_{12}^3}+\frac{1}{\rho_{22}^3}\right)+\right.$$

$$\left.\nu\left(\left(p-ak\right)\sin\theta_2+p\lambda_1\sin\theta_{12}\right)\left(\frac{1}{\rho_{11}^3}-\frac{1}{\rho_{21}^3}\right)\right]-2p\left(1+\theta_2'\right)\lambda_2'+\frac{p^4}{C^2k^3m_1}T_1\sin\theta_{12}, \tag{25}$$

$$pk\lambda_1'' = aek\left(\cos f\cos\theta_1+2\sin f\sin\theta_1\right)+p\lambda_1-\frac{\nu\left(\left(-p+ak\right)\cos\theta_1+p\lambda_1\right)}{\rho_{11}^3}-$$

$$\frac{\mu\left(ak\cos\theta_1+p\lambda_1\right)}{\rho_{12}^3}+\left(-p\nu+ak\right)\cos\theta_1+pk\lambda_1\theta_1'\left(2+\theta_1'\right)-\frac{p^4}{C^2k^2m_1}\left(T_1-T_2\cos\theta_{12}\right) \tag{26}$$

$$pk\lambda_2'' = \nu\left(\left(-p+ak\right)\cos\theta_2+p\lambda_1\cos\theta_{12}\right)\left(\frac{1}{\rho_{11}^3}-\frac{1}{\rho_{21}^3}\right)+$$

$$\mu\left(ak\cos\theta_2+p\lambda_1\cos\theta_{12}\right)\left(\frac{1}{\rho_{12}^3}+\frac{1}{\rho_{22}^3}\right)+$$

$$p\lambda_2\left(\frac{\mu}{\rho_{22}^3}-\frac{\nu}{\rho_{21}^3}\right)-p\lambda_2+pk\lambda_2\theta_2'\left(2+\theta_2'\right)+\frac{p^4}{C^2k^2}\left(\frac{\left(\cos\theta_{12}T_1-T_2\right)}{m_1}-\frac{T_2}{m_2}\right) \tag{27}$$

where $\theta_{12}=\theta_1-\theta_2$,

$$\rho_{11}=\sqrt{\lambda_1^2\sin\theta_1^2+\left(\mu+\sigma-\lambda_1\cos\theta_1\right)^2}, \tag{28}$$

$$\rho_{12} = \sqrt{\lambda_1^2 \sin\theta_1^2 + \left(\nu - \sigma + \lambda_1 \cos\theta_1\right)^2}\,, \tag{29}$$

$$\rho_{21} = \sqrt{\left(\mu + \sigma - \lambda_1 \cos\theta_1 - \lambda_2 \cos\theta_2\right)^2 + \left(\lambda_1 \sin\theta_1 + \lambda_2 \sin\theta_2\right)^2}\,, \tag{30}$$

$$\rho_{22} = \sqrt{\left(\nu - \sigma + \lambda_1 \cos\theta_1 + \lambda_2 \cos\theta_2\right)^2 + \left(\lambda_1 \sin\theta_1 + \lambda_2 \sin\theta_2\right)^2} \tag{31}$$

The right-hand sides of equations Eqs. (24)-(27) clearly include the tension forces of the tethers T_1 and T_2. When the laws governing the change in tether lengths are known and specified as functions of time $l_1(t)$ and $l_2(t)$, Eqs. (24)-(27) enable the determination of the tension forces T_1 and T_2, as follows

$$T_1 = \frac{m_1 m_2}{m_1 + m_2 \sin\theta_{12}^2}\left[GM_1\left(-\frac{\left(l_1 + \rho_1\cos\theta_1\right)}{\mu\rho_{11}^3} - \right.\right.$$

$$\left.\left(\cos\theta_{12}\left(-\frac{\rho_1\cos\theta_2 + l_1\cos\theta_{12}}{\rho_{11}^3} + \frac{\rho_1\cos\theta_2 + l_1\cos\theta_{12} + l_2}{\rho_{21}^3}\right)\right)\right) +$$

$$GM_2\left(-\frac{\left(l_1 + \rho_2\cos\theta_1\right)}{\mu\rho_{12}^3} - \cos\theta_{12}\left(-\frac{\rho_2\cos\theta_2 + l_1\cos\theta_{12}}{\rho_{12}^3} + \frac{\rho_2\cos\theta_2 + l_1\cos\theta_{12} + l_2}{\rho_{22}^3}\right)\right) +$$

$$\left.\frac{1}{\mu}\left(a\omega^2\cos\theta_1 + l_1\left(\omega + \dot{\theta}_1\right)^2 - \ddot{l}_1\right) + l_2\cos\theta_{12}\left(\omega + \dot{\theta}_2\right)^2 - \cos\theta_{12}\ddot{l}_2\right], \tag{32}$$

$$T_2 = \frac{m_1 m_2}{m_1 + m_2 \sin\theta_{12}^2}\left[GM_1\left(\frac{\rho_1\sin\theta_1\sin\theta_{12}}{\rho_{11}^3} - \frac{\rho_1\cos\theta_2 + l_1\cos\theta_{12} + l_2}{\rho_{21}^3}\right) + \right.$$

$$GM_2\left(\frac{\rho_2\sin\theta_1\sin\theta_{12}}{\rho_{12}^3} - \frac{\rho_2\cos\theta_2 + l_1\cos\theta_{12} + l_2}{\rho_{22}^3}\right) +$$

$$\left.\frac{a\omega^2}{2}\left(\cos\left(2\theta_1 - \theta_2\right) + \cos\theta_2\right) + l_1\left(\omega + \dot{\theta}_1\right)^2\cos\theta_{12} + l_2\left(\omega + \dot{\theta}_2\right)^2 - \ddot{l}_1\cos\theta_{12} - \ddot{l}_2\right] \tag{33}$$

where $\rho_1 = a + p\mu$, $\rho_2 = a - p\nu$.

3. Two types of elevators anchored on Phobos below the L1 libration point

The following two types of anchored space elevators are considered:

1. A classic lunar-anchored space elevator concept, where the motion of a climber occurs between the surface of Phobos and a station, and it is clear that the centre of mass of the station-climber system must always be above the L1 libration point relative to the surface of Phobos (Fig. 2a). In this case the total length of the tether remains unchanged

$$l = l_1 + l_2 = const \tag{34}$$

This type of space elevator can be used to transport scientific equipment and samples from the station to the surface of Phobos and back. In addition, the station can be placed in a quasi-satellite orbit, which greatly expands the range of transport tasks that can be solved by such space elevator.

2. A new concept of a hovering lunar space elevator, where the station is anchored on a tether of constant length above the L1 libration point, and the tethered end-mass moves from the station towards Mars according to a determined law (Fig. 2b)

$$l_1 = const,\ l_2 = l_2(t) \tag{35}$$

Once the end-mass has reached a certain altitude, it can either become a stationary spacecraft between Mars and Phobos (Figs. 2b and 2c), or it can separate from the tether and go into free flight with the following initial conditions in the local-vertical–local-horizontal frame Oxy (Fig. 2c):

$$x = a - \left(l_1 + l_2\right),\ y = 0,\ \dot{x} = 0,\ \dot{y} = 0 \tag{36}$$

Depending on the separation altitude ($x = a - (l_1 + l_2)$), the space probe can free-float around Mars, including reaching the surface of Mars.

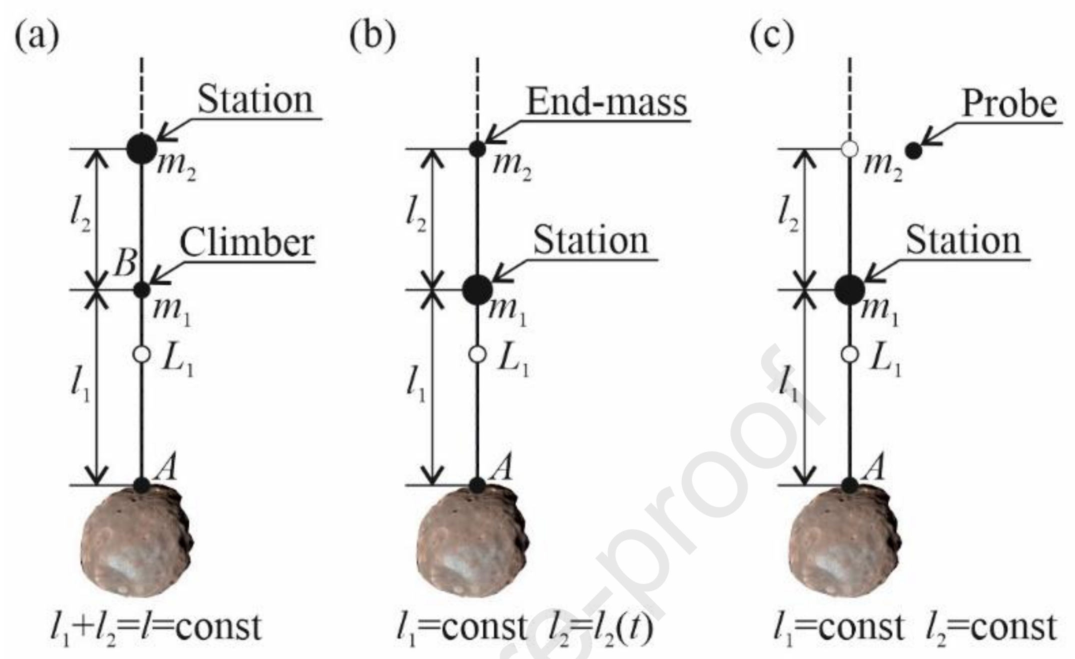

Fig. 2. (**a)** The standard space elevator, (**b)** the hovering space elevator and (**c)** the space floating probe.

Both types of space elevators described above can be modeled using the mathematical model of the space elevator presented in Section 2. Note that it is possible to study other similar missions using the proposed mathematical model.

4. The classical lunar space elevator

4.1. Ascent to the station

The ascent of the climber to the station consists of three phases: acceleration from zero velocity to a given velocity, the main phase of ascent at a constant velocity ($V = const$), and the braking phase, similar to that proposed by [34].

Accelerating phase $t \in (t_0, t_0 + t_V)$

$$l_1 = l_0 + \frac{4Vt_V}{\pi}\sin\left[\frac{\pi\left(t-t_0\right)}{4t_V}\right]^2 \tag{37}$$

$$(V_1 = \frac{d}{dt}l_1 = V\sin\left[\frac{\pi\left(t-t_0\right)}{2t_V}\right], W_1 = \frac{d}{dt}V_1 = \frac{\pi V}{2t_V}\cos\left[\frac{\pi\left(t-t_0\right)}{2t_V}\right])$$

Main phase $t \in \left(t_0 + t_V, t_f - t_V\right)$

$$l_1 = l_0 + V\left[t - t_0 - t_V\left(1 - \frac{2}{\pi}\right)\right] \tag{38}$$

Decelerating phase $t \in \left(t_f - t_V, t_f\right)$

$$l_1 = l_0 + \left(t_f - t_0 - 2t_V\right)V + \frac{4Vt_V}{\pi}\cos\left[\frac{\pi\left(t-t_f\right)}{4t_V}\right]^2 \tag{39}$$

$$(V_1 = \frac{d}{dt}l_1 = -V\sin\left[\frac{\pi\left(t_f-t\right)}{2t_V}\right], W_1 = \frac{d}{dt}V_1 = -\frac{\pi V}{2t_V}\cos\left[\frac{\pi\left(t_f-t\right)}{2t_V}\right])$$

where l_0 is small length of the tether l_1, at the initial moment of time t_0, t_f is the end time, t_V is the time corresponding to the acceleration and deceleration phases. Fig. 3 plots the tethers' deflection angles θ_1, θ_2 and the tensions T_1 and T_2, when the climber and the station have the masses

$$m_1 = 10\,kg,\ m_2 = 100\,kg \tag{40}$$

The climber's velocity is

$$V = 0.5\,m s^{-1} \tag{41}$$

The following initial conditions are used for simulation

$$\theta_1 = 0.1rad,\ \theta_2 = -0.1rad,\ \dot{\theta}_1 = 0,\ \dot{\theta}_2 = 0 \tag{42}$$

The space elevator's total length is

$$l = l_1 + l_2 = 100\,km \tag{43}$$

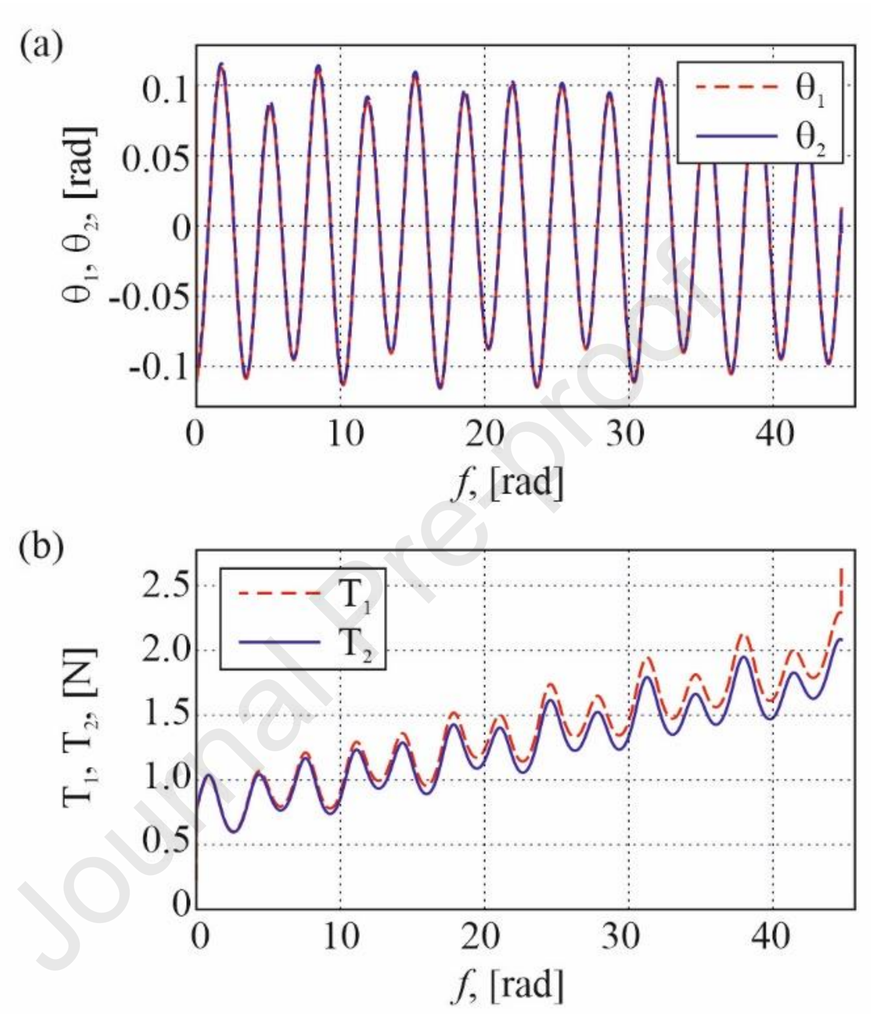

Fig. 3. **(a)** The tethers' deflection angles θ_1, θ_2 and **(b)** the tether tensions T_1 and T_2 for the phases duration $t_V = 25\,s$.

The oscillations of the tether remain close to the initial values, as shown in Fig. 3, and the tether tension force reaches values of about 2.5 N at the final braking section of the climber.

4.2. Descent from the station

The three phases of a climber's descent from the station to Phobos are as follows:

Accelerating phase $t \in \left(t_0, t_0 + t_V\right)$

$$l_1 = l - l_0 + \frac{4Vt_V}{\pi}\sin\left[\frac{\pi\left(t - t_0\right)}{4t_V}\right]^2 \tag{44}$$

$$(V_1 = \frac{d}{dt}l_1 = V\sin\left[\frac{\pi\left(t-t_0\right)}{2t_V}\right], \quad W_1 = \frac{d}{dt}V_1 = \frac{\pi V}{2t_V}\cos\left[\frac{\pi\left(t-t_0\right)}{2t_V}\right])$$

Main phase $t \in \left(t_0 + t_V, t_f - t_V\right)$

$$l_1 = l - l_0 + V\left[t - t_0 - t_V\left(1 - \frac{2}{\pi}\right)\right] \tag{45}$$

Decelerating phase $t \in \left(t_f - t_V, t_f\right)$

$$l_1 = l - l_0 + \left(t_f - t_0 - 2t_V\right)V + \frac{4Vt_V}{\pi}\cos\left[\frac{\pi\left(t - t_f\right)}{4t_V}\right]^2 \tag{46}$$

$$(V_1 = \frac{d}{dt}l_1 = -V\sin\left[\frac{\pi\left(t_f - t\right)}{2t_V}\right], W_1 = \frac{d}{dt}V_1 = -\frac{\pi V}{2t_V}\cos\left[\frac{\pi\left(t_f - t\right)}{2t_V}\right])$$

Fig. 4 illustrates the descent of a climber at a velocity of

$$V = -0.5ms^{-1} \tag{47}$$

The tether vibrations remain within the limits close to the initial values and the tether tension force does not exceed 2.5 N. The masses of climber and station, the initial conditions of motion and the total length of the space elevator are determined as in the case of ascent by expressions (40), (42) and (43).

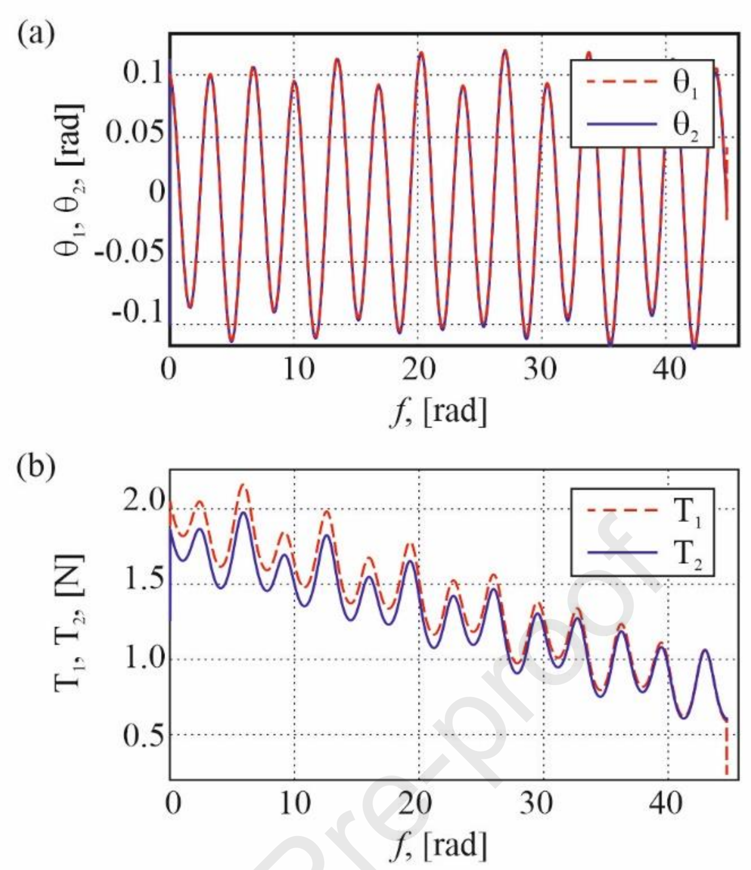

Fig. 4. (**a**) The deflection angles of the tether θ_1, θ_2 and (**b**) the tether tension T_1 and T_2 for the acceleration and deceleration phases duration $t_V = 25s$.

5. Ascent of the end-mass above the station along the primary line

5.1. Preliminary comments

Consider a space elevator where the station is anchored to a tether of constant length ($l_1 = const$) and is located above of the L1 libration point relative to Phobos, so that the tether l_1 is always taut. The tether l_2 can now be deployed towards Mars. In this case, the station is now labelled as m_1 and the end-mass is labelled as m_2 (Fig. 2b). In the following, the primary line is the line connecting the two primary bodies (Mars-Phobos). It is clear that if the length of the tether l_2 changes slowly, the tether's oscillation amplitude oscillations will also change slowly, i.e. adiabatically. Approximate analytical law for the variation of oscillation amplitude of the tether is obtained below and compared with the solution obtained by numerical integration of Eqs. (24) and (25).

5.2. Adiabatic invariant and approximate analytical solution for the amplitude of the tether oscillation

Adiabatic invariants [37-40] find applications in many fields, and the underlying ideas, such as averaging methods, are used in the study of oscillating systems with slowly varying parameters, for example, to determine the envelope of the angle of attack during spacecraft re-entry [41]. Let us introduce assumptions that allow to obtain the required adiabatic invariant without distorting the physical picture of the process under study:

1. The mass of the station is much greater than the mass of the end-mass

$$m_2 / m_1 \ll 1 \tag{48}$$

2. The circular restricted three-body problem is considered.

3. Due to the condition (48), the end-mass has little effect on the behaviour of the station, and the station can then be assumed to be stationary on the primary line

$$\theta_1 = 0 \qquad (l_1 = const) \tag{49}$$

4. The angles of the tether l_2 deflection are small

$$\theta_2 \ll 1 \tag{50}$$

5. The end-mass velocity is low

$$\varepsilon = \frac{V}{nb} \ll 1 \tag{51}$$

where n is mean orbital rate, ε is the small dimensionless parameter, $b = a - l_1$ is the coordinate of the B point of attachment of the space elevator in the frame Oxy (Fig. 2b).

The equations of motion (24)-(27) include the tether tension forces (32)-(33), their exclusion from the equations is a separate complex problem, the solution of which leads to cumbersome equations of little use for further analytical calculations. Therefore, the Lagrange formalism is used below to derive equations of motion that do not explicitly include the tension forces.

On the basis of the above assumptions, this space elevator can be thought of as a pendulum of variable length, fixed at a point on the primary line, which is far from the surface of Phobos at a distance of l_1. The equations of plane motion of the variable length pendulum can be obtained in the frame Oxy using the Lagrange formalism

$$\frac{d}{dt}\frac{\partial L}{\partial \dot{\theta}} - \frac{\partial L}{\partial \theta} = 0, \quad \frac{d}{dt}\frac{\partial L}{\partial \dot{l}} - \frac{\partial L}{\partial l} = 0 \qquad (\theta \equiv \theta_2,\ l \equiv l_2) \tag{52}$$

where L is the Lagrangian. The position of the end-mass can be determined as

$$\mathbf{r} = (b - l\cos\theta, -l\sin\theta, 0)^T, \tag{53}$$

The velocity of the end-mass in the inertial coordinate system can be found as

$$\mathbf{V}_I = \frac{d\mathbf{r}}{dt} + \mathbf{n} \times \mathbf{r} \tag{54}$$

where $\mathbf{n} = (0,0,n)^T$ is the mean orbital rate vector. The Lagrangian function can be found as

$$L = T - U \tag{55}$$

where T is the kinetic energy of the systems, U is the potential energy.

$$T = \frac{m}{2}\mathbf{V}_I \cdot \mathbf{V}_I \tag{56}$$

$$U = -Gm\left[\frac{M_1}{\sqrt{(\mathbf{r}-\mathbf{R}_1)\cdot(\mathbf{r}-\mathbf{R}_1)}} + \frac{M_2}{\sqrt{(\mathbf{r}-\mathbf{R}_2)\cdot(\mathbf{r}-\mathbf{R}_2)}}\right] \tag{57}$$

$$\mathbf{R}_1 = (-\mu p, 0, 0)^T,\ \ \mathbf{R}_2 = (\nu p, 0, 0)^T \tag{58}$$

where $m \equiv m_2$, p is the distance between the primaries. Eqs. (52), taking into account (55), (56) and (57) can be expressed as follows

$$l\ddot{\theta} + \frac{GM_1(b+p\mu)\sin\theta}{r_1^3} + \frac{GM_2(b-p\nu)\sin\theta}{r_2^3} - bn^2\sin\theta + 2\dot{l}\left(n+\dot{\theta}\right) = 0 \tag{59}$$

$$\ddot{l} + \frac{GM_1\left(l-(b+p\mu)\cos\theta\right)}{r_1^3} + \frac{GM_2\left(l-(b-p\nu)\cos\theta\right)}{r_2^3} + bn^2\cos\theta - l\left(n+\dot{\theta}\right)^2 = 0 \tag{60}$$

where

$$r_1 = \sqrt{l^2 + (b+p\mu)^2 - 2l(b+p\mu)\cos\theta},\ r_2 = \sqrt{l^2 + (b-p\nu)^2 - 2l(b-p\nu)\cos\theta} \tag{61}$$

Assuming that the law of variation of the tether length is given as a known function of time

$$l = l(t) \tag{62}$$

then for small angles $\theta \ll 1$ equation of the pendulum (59) can be written down as follows

$$\ddot{\theta} + \omega^2\theta = 0 \tag{63}$$

where the frequency of oscillation is

$$\omega(l)=\sqrt{\frac{1}{l}\left[\frac{GM_1(b+p\mu)}{(b+p\mu-l)^3}+\frac{GM_2(b-p\nu)}{(b-p\nu-l)^3}-bn^2\right]} \tag{64}$$

The expression in brackets is the sum of the forces acting on the end-mass: the gravitational force of Mars, the gravitational force of Phobos, the centrifugal force in the frame Oxy. This sum is positive because the station is above the L1 libration point relative to Phobos. In general, a second-order linear differential equation of the pendulum type (63) with a slowly varying frequency is not integrable in quadrature and is rather difficult to study. However, if the frequency changes slowly

$$\frac{d\omega}{dt}=\frac{d\omega}{dl}V=\varepsilon\frac{d\omega}{dl}bn\,, \tag{65}$$

such a study can be carried out using the concept of the adiabatic invariant [34-37]

$$J=\oint p_\theta d\theta=const \tag{66}$$

The generalised impulse is defined as

$$p_\theta=\frac{\partial L}{\partial\theta}=l^2\dot{\theta} \tag{67}$$

where the Lagrangian corresponding to Eq. (63) is

$$L=l^2\frac{\dot{\theta}^2}{2}+\omega^2l^2\frac{\theta^2}{2} \tag{68}$$

The solution of Eq. (63) is written as

$$\theta=A\sin\omega t \tag{69}$$

Substituting this solution into Eq. (66) gives the adiabatic invariant in the form

$$J=l^2\oint\dot{\theta}^2dt=A^2l^2\omega=const \tag{70}$$

The amplitude of the oscillation as a function of the length of the pendulum is therefore

$$A(l)=\frac{C}{\sqrt{l^2\omega(l)}}=\frac{C}{\sqrt[4]{l^3\left[\frac{GM_1(b+p\mu)}{(b+p\mu-l)^3}+\frac{GM_2(b-p\nu)}{(b-p\nu-l)^3}-bn^2\right]}} \tag{71}$$

where $C>0$ is a positive constant, which is determined taking into account the initial conditions. Eq. (71) could also be obtained by following the calculations [39, pp. 55-56].

If point B is above L1 of the libration point $b<x_{L_1}$ (Fig. 2b) and the length of the tether does not exceed $l<(b+p\mu)$, then the partial derivative of the amplitude (71) with respect to the length of the tether is less than zero

$$\frac{\partial A}{\partial l}=-\frac{3C}{4}\frac{Gl\left[\frac{M_1(b+p\mu)}{(b+p\mu-l)^4}+\frac{M_2(b-p\nu)}{(b-p\nu-l)^4}\right]+\left[\frac{GM_1(b+p\mu)}{(b+p\mu-l)^3}+\frac{GM_2(b-p\nu)}{(b-p\nu-l)^3}-bn^2\right]}{l^{7/4}\left[\frac{GM_1(b+p\mu)}{(b+p\mu-l)^3}+\frac{GM_2(b-p\nu)}{(b-p\nu-l)^3}-bn^2\right]^{5/4}} \tag{72}$$

It is clear that as the length of the tether increases

$$\frac{dl}{dt}=V>0, \tag{73}$$

the amplitude of the tether oscillations decreases, and vice versa, as the length of the tether decreases, the amplitude of the tether oscillations increases.

5.3. Simulation of the end-mass ascent

Fig. 5b shows the angles of the tether deflection θ_1, θ_2 and the tether tensions T_1 and T_2, and also the amplitude of the oscillations of the tether l_2, calculated by the approximate formula (71), when the masses of the station and the end-mass are equal, respectively

$$m_1 = 100\,kg\,,\; m_2 = 10\,kg \tag{74}$$

The end-mass velocity is

$$V = 0.5\,m\,s^{-1} \tag{75}$$

for the following initial conditions:

$$\theta_1 = 0.1rad\;,\; \theta_2 = -0.1rad\,,\; \dot{\theta}_1 = 0\,,\; \dot{\theta}_2 = 0 \tag{76}$$

The station is fixed at a height above the surface of Phobos $l_1 = 10\,km$, and the tether with the end-mass at the end will be deployed from a distance of $l_2 = 1500\,km$ from the station towards Mars. The three phases of tether l_2 deployment are similar to the three phases of tether l_1 deployment, as determined by Eqs. (37)-(39).

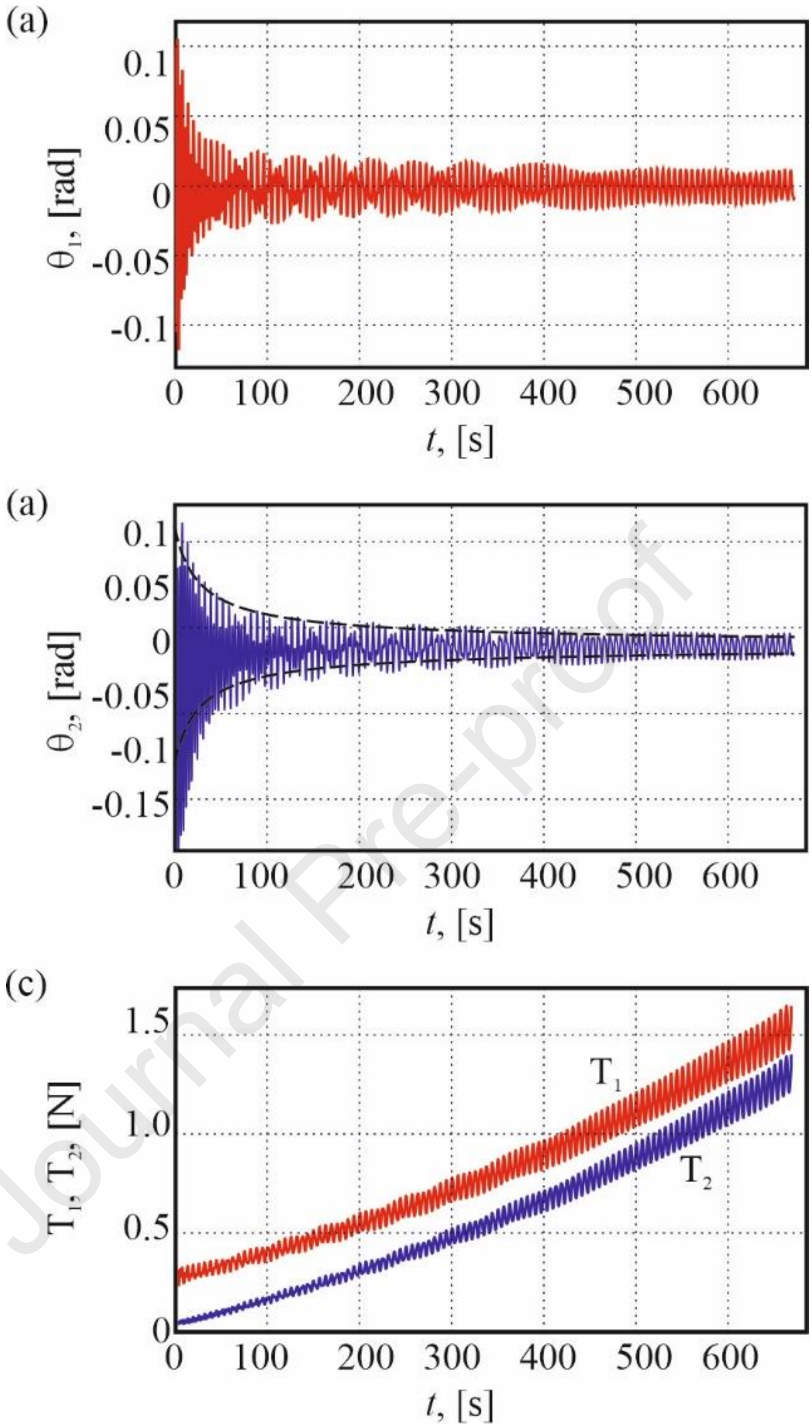

Fig. 5. **(a)** The deflection tether angle θ_1, **(b)** the deflection tether angle θ_2, and the amplitude of the oscillation A and $-A$, **(c)** the tether tensions T_1 and T_2 for duration of the phases $t_V = 200\,s$.

Three points can be made from the graphs in Fig. 5:

- Fig. 5a. During the tether l_2 deployment, the oscillations of not only the tether l_2 but also the tether l_1 are damped.

- Fig. 5b. The obtained approximate analytical solution (71) shows a good qualitative agreement with the results of the numerical integration of Eqs. (24) and (25).

- Fig. 5c. The tension force of both tethers increases when the tether is deployed and does not exceed 2 N.

5.4. Simulation of the end-mass descent

The end-mass can return to the station by retracting the tether l_2. When simulating the motion of the space elevator, the end-mass velocity during the main phase of the descent is set to

$$V = -0.5 m s^{-1} \tag{77}$$

The three phases of tether l_2 retraction are similar to the three phases of tether l_1 deployment, as determined by Eqs. (44)-(46). The station is fixed high above the surface of Phobos $l_1 = 10 km$, and tether l_2 with the end-mass is deployed 250 km from the station towards Mars. The masses of the station and the end-mass and the initial conditions of motion are taken as in the case of the end-mass ascent according to formulas (74) and (76). Fig. 6 shows the results of the numerical integration of the space elevator equations of motion (24)-(27).

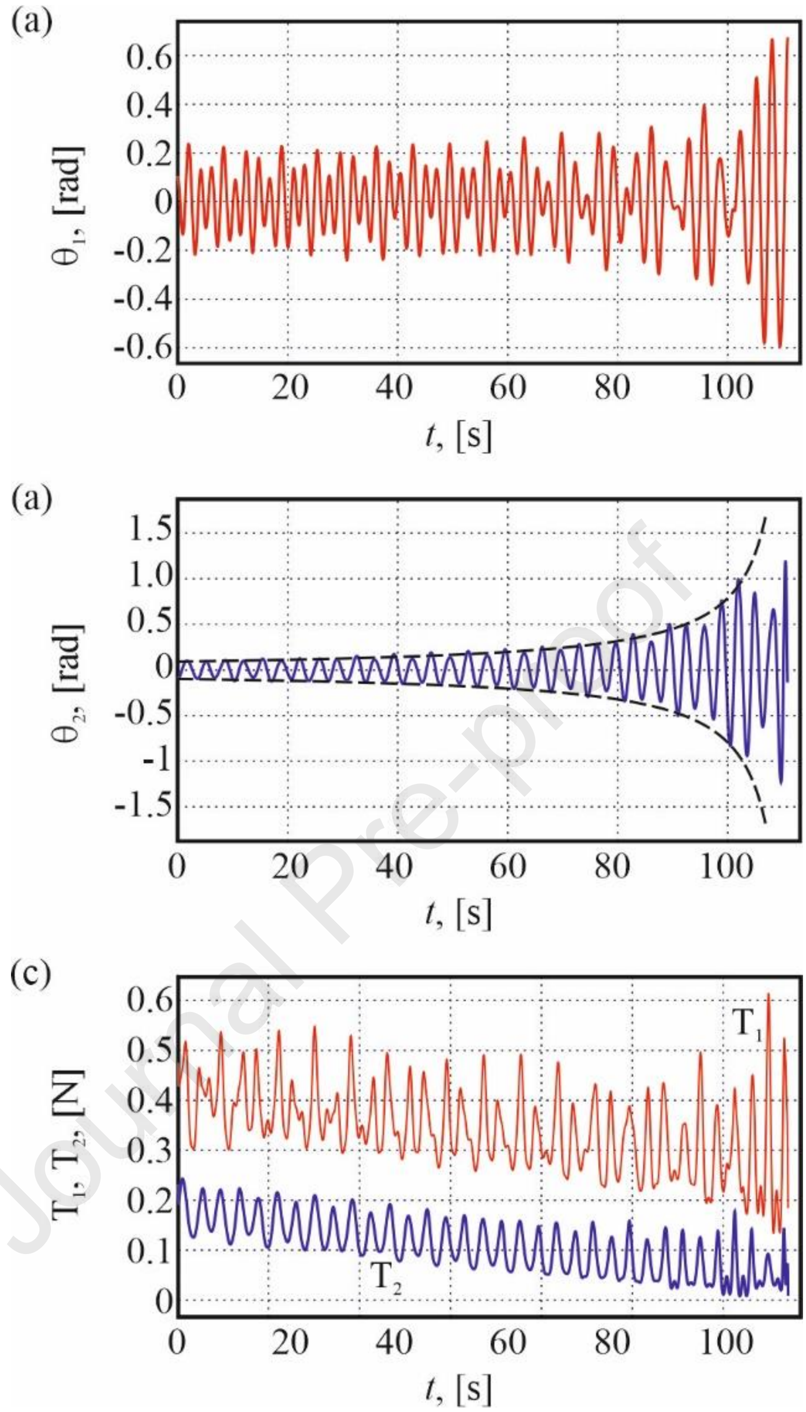

Fig. 6. (**a**) The deflection tether angle θ_1, (**b**) the deflection tether angle θ_2, and the amplitude of the oscillation A and $-A$, (**c**) the tether tension T_1 and T_2 for duration of the phases $t_V = 200\,s$.

Note that for tether l_2 length of 250 km, the amplitude of the oscillations increases to values of 1 rad (Fig. 6b) as the end-mass approaches the station; for the longer tether length, the amplitude increases with subsequent winding of the tether

l_2 onto the station. To prevent this phenomenon, additional devices are required, such as small engines as described in [42].

6. Flight trajectories and descent of a probe to Mars

Consider the case where, on this second space elevator type, the end-mass (or a probe) separates from the tether after reaching the endpoint. It is assumed that at the moment of separation the probe is on the primary line and its velocity in the frame Oxy is zero. The simulations are carried out by numerical integration of the classical equations of free motion in the context of the planar circular restricted three-body problem [35] for the initial conditions (36). Depending on the separation height of the climber ($y = l_1 + l_2, l_1 = const$), i.e., the length of tether l_2, different pictures with different periods and heights of Mars circling (Figs. 7a, 7b, 7c), or descent to the surface of Mars (Fig. 7d) are observed. The trajectory of the descent to Mars is shown without taking into account aerodynamic forces.

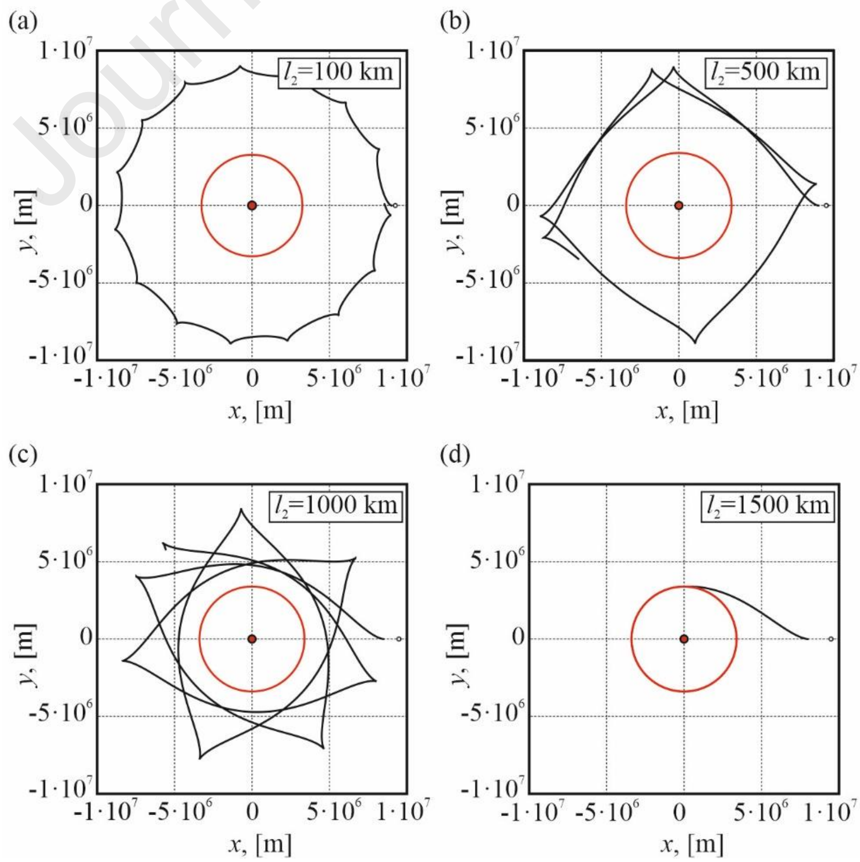

Fig. 7. Probe trajectories as a function of the length of tether l_2.

It can be seen, firstly, that there are points on the overflight trajectories (Figs. 7a-7c) where the velocity of the climber (probe) is zero, including the initial point, and, secondly, that the trajectories of the descent to Mars, such as the one shown in Fig. 7d, depend on the length of the tether l_2 at which the climber separates from the tether.

6. Conclusions

The space elevator anchored to Phobos under the L1 libration point is considered in the framework of the planar restricted elliptic three-body problem. The main results of the paper can be reduced to a few points:

1. The principal possibility of functioning an anchored elevator below the L1 libration point of two configurations of the Mars-Phobos system is shown:
   - a classical configuration, when the climber is below the station, i.e., between the surface of Phobos and the station.
   - a new configuration, when the end-mass is above the station of space elevator.

   In the first case, the length of the space elevator remains unchanged, whereas in the second case, the length of the space elevator increases when the tether with the climber attached is released and decreases when the tether is retracted. In both cases, the station is located above L1 of the libration point to ensure tether tension.
2. The law of the climber motion is chosen to ensure that the tethers are tensioned as the climber moves.
3. Using the concept of adiabatic invariant, it is shown analytically and confirmed by numerical modelling that the oscillations of the tether are damped when the second configuration of space elevator is deployed, while the amplitude of the oscillations increases when it is retracted. The second circumstance limits the length of the space elevator if it needs to retract.

4. It is shown that the second type of space elevator with a free end can be used as a stationary probe (in the Local-Vertical-Local-Horizontal frame Oxy), fixed at a given distance between Mars and Phobos, and a means of launching a probe on a fly-around trajectory and a descent trajectory to the surface of Mars.

Obviously, these preliminary analytical and numerical studies of the functioning of the space elevator anchored to Phobos do not exhaust all the possibilities of implementation of the proposed concepts.

Declaration of competing interest

No potential conflict of interest was reported by the authors.

Acknowledgments

I would like to thank Dr. Alexander Ledkov for helpful discussions of the results.

References

[1] K.E. Tsiolkovsky, Speculations between earth and sky. Isd-vo An-SSR, 1895, pp. 35.

{2] Y. Artsutanov, To Space by a Locomotive. Komsomolskaya Pravda, 31, Moscow, 1960, 946-947.

[3] J. Pearson, The orbital tower: a spacecraft launcher using the earth's rotational energy. Acta Astronaut. 2 (1975), 785–799.

[4] J. Huang, A.K. Misra, Controlled deployment of a long tether to operate as a partial space elevator, Astrodynamics 8 (2, SI) (2024) 311–321, http://dx.doi.org/10.1007/s42064-024-0225-5.

[5] A.K. Misra, S. Cohen, Space elevator—A revolutionary space transportation system, Mech. Sci. (1) (2021) 105–120, http://dx.doi.org/10.1007/978-981-15-5712-5_5.

[6] S.S. Cohen, A.K. Misra, The effect of climber transit on the space elevator dynamics, Acta Astronaut. 64 (5) (2009) 538–553, http://dx.doi.org/10.1016/j.actaastro.2008.10.003.

[7] S.S. Cohen, A.K., Misra, Elastic oscillations of the space elevator ribbon, J. Guid. Control. Dyn. 30 (2007) 1711–1717, https://doi.org/10.2514/1.29010.

[8] A.K. Misra, Z. Amier, V.J. Modi, Attitude dynamics of three-body tethered systems, Acta Astronaut. 17(10) (1988) 1059–1068, https://doi.org/10.1016/0094-5765(88)90189-0.

[9] P. Woo, A.K. Misra, Dynamics of a partial space elevator with multiple climbers, Acta Astronaut. 67(7–8) (2010) 753–763, https://doi.org/10.1016/j.actaastro.2010.04.023.

[10] P. Woo, A.K. Misra, Energy considerations in the partial space elevator, Acta Astronaut. 99 {2014) 78–84, https://doi.org/10.1016/j.actaastro.2014.02.013.

[11] G. Shi, Z.H. Zhu, Cooperative game-based multi-objective optimization of cargo transportation with floating partial space elevator, Acta Astronaut. 205 (2023) 110-118, https://doi.org/10.1016/j.actaastro.2023.01.024.

[12] G. Shi, Z.H. Zhu, Prescribed performance based dual-loop control strategy for configuration keeping of partial space elevator in cargo transportation, Acta Astronaut. 189 (2021) 241-249, https://doi.org/10.1016/j.actaastro.2021.08.056.

[13] G. Shi, Z.H. Zhu, Orbital radius keeping of floating partial space elevator in cargo transposition. Astrodynamics 7(3) (2023) 259–269, https://doi.org/10.1007/s42064-022-0156-y.

[14] G. Shi, Z.H. Zhu, New geometric formulation for libration dynamics and suppression of partial space elevator by fuzzy logic and thrust vectoring control, Acta Astronaut. 217(2024) 293-301, https://doi.org/10.1016/j.actaastro.2024.02.005.

[15] M. Kakavand, Z.H. Zhu, Rigid-flexible coupled dynamics and configuration stability of maneuverable space tether net under impact loads, Acta Astronaut. 232 (2025) 114-131, https://doi.org/10.1016/j.actaastro.2025.02.031.

[16] J. Pearson, Anchored lunar satellites for cislunar transportation and communication, J. of the Astronautical Sciences, 27(1) (1979) 39-62.

[17] B. Wang, Z. Meng, P. Huang, Attitude control of towed space debris using only tether, Acta Astronaut. 138 (SI) (2017) 152–167, http://dx.doi.org/10.1016/j.actaastro.2017.05.012.

[18] F. Zhang, P. Huang, A novel underactuated control scheme for deployment/retrieval of space tethered system, Nonlinear Dynam. 95 (4) (2019) 3465–3476, http://dx.doi.org/10.1007/s11071-019-04767-3.

[19] D. Bourabah, E.M. Botta, Length-rate control for libration reduction during retraction of tethered satellite systems, Acta Astronaut. 201 (2022) 152-163, https://doi.org/10.1016/j.actaastro.2022.08.037.

[20] E.M. Botta, I. Sharf, A.K. Misra, M. Teichmann, On the simulation of tether-nets for space debris capture with vortex dynamics, Acta Astronaut. 123 (2016) 91–102, http://dx.doi.org/10.1016/j.actaastro.2016.02.012.

[21]Y. Lu, Z. Jia, X. Liu, K. Lu, Output feedback fault-tolerant control for hypersonic flight vehicles with non-affine actuator faults, Acta Astronaut. 193 (2022) 324-337, https://doi.org/10.1016/j.actaastro.2022.01.023.

[22] D.H.Wright, L. Bartoszek, A.J. Burke, D. Dotson, H. El Chab, J. Knapman, et al., Conditions at the interface between the space elevator tether and its climber, Acta Astronaut. 211 (2023) 631-649, https://doi.org/10.1016/j.actaastro.2023.06.047.

[23] Q. Li, Z. Meng, C. Jia, Chain tethered satellite formation reconfiguration: An event-triggered practical prescribed-time control approach. Acta Astronautica, 224 (2024) 436-444. https://doi.org/10.1016/j.actaastro.2024.08.028.

[24] C. Liu, S. Chen, Y. Guo, W. Wang, Robust adaptive control for rotational deployment of an underactuated tethered satellite system. Acta Astronaut. 203 (2023) 65-77. https://doi.org/10.1016/j.actaastro.2022.11.025.

[25] R. Kuzuno, S. Dong, Y. Takahashi, T. Okada, C. Xue, K. Otsuka, K. Makihara, High-fidelity flexible multibody model considering torsional deformation for nonequatorial space elevator, Acta Astronaut. 220 (2024) 504-515, https://doi.org/10.1016/j.actaastro.2024.05.008.

[26] Q. Li, Z. Meng, C. Jia, Chain tethered satellite formation reconfiguration: An event-triggered practical prescribed-time control approach, Acta Astronaut. 224 (2024) 436-444, https://doi.org/10.1016/j.actaastro.2024.08.028

[27] W. Zhigang, W. Weiwei, L. Lu, L. Jiafu, Dynamic simulation of cargo transport along cislunar suspension tether by single node coupling model, Acta Astronaut. 226 (2025) 262-274, https://doi.org/10.1016/j.actaastro.2024.10.050.

[28] M.P. Cartmell, D.J. McKenzie, A review of space tether research. Prog. Aerosp. Sci. 44(1) (2008) 1–21, https://doi.org/10.1016/j.paerosci.2007.08.002.

[29] K. Kempton, J. Pearson, E. Levin, J. Carroll, F. Amzajerdian, Phase 1 Study for the Phobos L1 Operational Tether Experiment (PHLOTE), End Report (2018) pp. 1–91. NASA, https://ntrs.nasa.gov/search.jsp?R=20190000916

[30] V.V. Beletsky, E.V. Levin, Dynamics of Space Tether Systems, Univelt Incorporated, San Diego (1993).

[31] E.M. Levin, Dynamic Analysis of Space Tether Missions, Univelt Incorporated, San Diego (2007).

[32] V. Aslanov, Prospects of a tether system deployed at the L1 libration point, Nonlinear Dyn. 106 (2021) 2021–2033, https://doi.org/10.1007/s11071-021-06884-4Пр0.1007/s11071-023-09108-z.

[33] V. Aslanov, Suppressing chaotic oscillations of a tether anchored to the Phobos surface under the L1 libration point. Chaos, Solitons & Fractals, 181 (2024) 114663, https://doi.org/10.1016/j.chaos.2024.114663

[34]V. Aslanov, A space elevator deployed at the L1 Mars–Phobos libration point. Nonlinear Dyn 112 (2024) 1–11, https://doi.org/10.1007/s11071-024-09762-x.

[35] V. Szebehely, The Restricted Problem of Three Bodies, Academic Press Inc., New York (1967).

[36] A.P. Markeev, Libration Points in Celestial Mechanics and Astrodynamics, Nauka, Moscow [in Russian] (1978).

[37] P. Ehrenfest, Adiabatische invarianten und quantentheorie. Annalen der Physik, 356(19), 327-352 (1916).

[38] J. M. Burgers, Die adiabatischen Invarianten bedingt periodischer Systeme. Ann. Physik, 52, 195 (1917).

[39] M. Born, The mechanics of the atom (1927).

[40] P.A.M. Dirac, The adiabatic invariance of the quantum integrals. Proceedings of the Royal Society of London. Series A, Containing Papers of a Mathematical and Physical Character, 107(744) (1925) 725-734.

[41] V. Aslanov, Rigid body dynamics for space applications. Butterworth-Heinemann (2017).

[42] V. Aslanov, Tether System in Martian-Moons-eXploration-Like Mission for Phobos Surface Exploration. Journal of Spacecraft and Rockets, 61(1) (2024) 319-326, https://doi.org/10.2514/1.A35777.

Declaration of Interest Statement

☒ The authors declare that they have no known competing financial interests or personal relationships that could have appeared to influence the work reported in this paper.

☐ The author is an Editorial Board Member/Editor-in-Chief/Associate Editor/Guest Editor for this journal and was not involved in the editorial review or the decision to publish this article.

☐ The authors declare the following financial interests/personal relationships which may be considered as potential competing interests: